The Flowfield in a Suddenly Enlarged Combustion Chamber

B. T. Yang* and M. H. Yu†
National Tsing-Hua University, Taiwan, Republic of China

The characteristics and dynamics of an abruptly expanded flow in a model combustion chamber (combustor) were investigated experimentally. The combustion chamber consisted of a plexiglass, circular duct with a suddenly enlarged section followed by a nozzle. The Reynolds number, based on the inlet duct diameter and center velocity, was 6.4×10^4. The wall pressure measurements were carried out with a laser-Doppler anemometer (LDA). Detailed profiles of mean velocities, turbulent intensities, turbulent shear stresses, and wall pressure distribution were developed. The dividing streamline, the reattachment point, and the magnitudes of the mean kinetic energy and turbulent kinetic energy were also determined.

I. Introduction

IN recent years, the integral rocket-ramjet has emerged as a new air-breathing propulsion system.[1] This device includes a rocket booster and ramjet engine and operates as a complete system. The rocket booster, carrying its own oxidizer, is designed to operate as a solid-propellant rocket in the initial stage of flight. After the rocket reaches a desirable flying speed, the nozzle and other components can be jettisoned. Then the ramjet engine is ignited to provide the necessary propulsion as the ram pressure achieves its optimal value.

The basic ramjet combustor configuration is the so-called sudden-expansion dump-type combustor. In this type of combustor, fuel injection occurs in the air inlet duct upstream of the dump station. Primary flame stabilization is provided by the flow-recirculation region just downstream of the dump section. The high turbulent intensities in this region increase the mixing of the fuel and air; thus combustion is more nearly complete.

The flowfield of abrupt axisymmetric expansion is a complicated phenomenon characterized by flow separation, flow recirculation, and flow reattachment. Such a flowfield may be divided by a dividing streamline (actually a dividing surface) into two main regions,[2] one being the flow-recirculation region, the other being the main flow region (as illustrated in Fig. 1). The point at which the dividing streamline strikes the wall is called the reattachment point. In the recirculation region, the high adverse pressure gradient results in reverse flow and promotes instability and turbulence. Between the main flow and the reverse flow along the wall, a new shear layer starts to grow.[3] Eddies produced in the recirculation region and in the neighborhood of the reattachment point can be considered as a highly concentrated source of turbulence. The subsequent convection, diffusion, and decay of the turbulent eddies have a dominant influence on the characteristics of mean motion. As to the reattachment length, according to Drewry,[2] it ranges between 7.9 and 9.2 step heights for Reynolds numbers between 1.3×10^6 and 2.2×10^6. The relation between the reattachment length and Reynolds number was also investigated by Bach and Roschke.[4] They found that at higher Reynolds numbers the reattachment length is a weak function of Reynolds number.

The step height h, the radius difference of the enlargement, is an important parameter for combustion chamber flow characterization. It determines how far the new shear layer that borders the reverse-flow region spreads into the original shear layer. In the present study, the step height was 0.314 combustion chamber diameter. The Reynolds number, based on the inlet duct diameter and central velocity, was 6.4×10^4. The inlet flow Mach number is another interesting parameter. Although the desirable flight Mach number of the ramjet is in the range of 2 to 5,[5] the present turbulence investigation involves a subsonic flow since the flowfield is a weak function of the Reynolds number.

The complexity of the flow configuration precluded any analytic solutions, so the investigation was carried out experimentally. The experimental study presented here was thus aimed to provide a set of precise observations for understanding the kinetics of the flowfield. Furthermore, it may offer researchers a unique flow condition with which to compare their numerical results.

II. Experimental Equipment and Procedure

Combustion Chamber Model

Figure 2 illustrates the flow system and the configuration of the combustion chamber model. The compressed airflow was supplied with a blower (3300 rpm/3 phase/1 kW). The flow was seeded with small water particles 3μm or smaller. Because of the need to conserve water droplets, the flow system formed a closed loop. These droplets were released into the flow at the bend and carried into the combustion chamber.

The combustion model was made of a 5-mm plexiglass. It consisted of an intake, a circular chamber, followed by a nozzle, as shown in Fig. 2. The length/diameter ratio L/D_2 for the combustor duct was 3.57. The step height was 0.314 D_2. Pressure taps (1-mm in diameter) were machined onto the combustor wall at 1-cm intervals, beginning at 3 cm from the inlet. These taps were used for wall pressure measurements. A wooden frame was used for adjusting and locking the positions of the model and, consequently, the measurement points.

Instrumentation

The instrumentation is plotted in Fig. 3. The velocity measurements were taken with a TSI 9100-3 laser-Doppler anemometer (LDA) system. A linearly polarized 15-mW helium-neon laser (wavelength 6328 Å) provided the coherent light source. This beam was split into two parallel beams by a beamsplitter. For the dual-beam mode, the intensity was equally divided. A Bragg cell with an oscillating frequency of 40 MHz was used to cause a 40-MHz frequency shift on the lower beam. It also formed a "moving fringe" pattern at the measuring point so that the reverse flow might be detected. The resulting pair of beams was then passed through a 25-cm focal-length lens at a beam separation distance of 5 cm. The

Received July 23, 1981; revision received March 25, 1982.

*Professor, Power Mechanical Engineering Department. Present address: Santa Barbara Engineering and Science Company, Isla Vista, Calif. Member AIAA.

†Research Assistant.

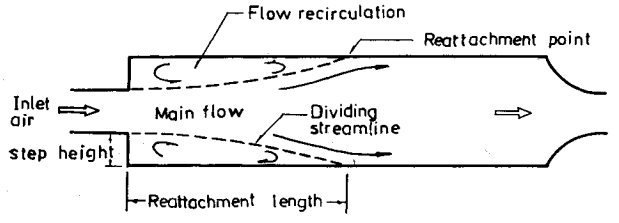

Fig. 1 Schematic illustration of a dump combustor flowfield.

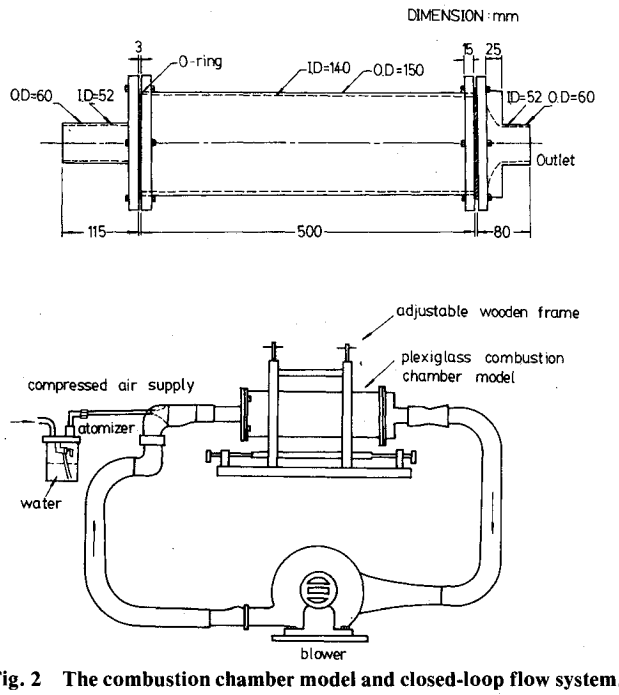

Fig. 2 The combustion chamber model and closed-loop flow system.

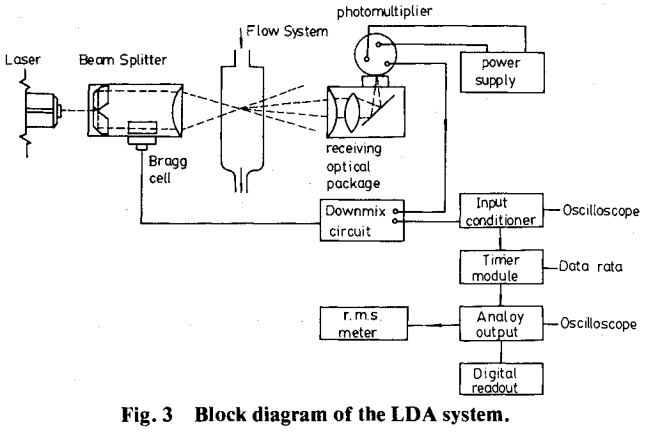

Fig. 3 Block diagram of the LDA system.

resulting beam intersection semiangle κ was 5.53 deg. When the beams crossed, they interfered with each other to form bright and dark "fringes." The fringe spacing d_f, a function of the laser wavelength λ and the half-angle of the beam intersection κ, can be computed from

$$d_f = \frac{\lambda}{2\sin\kappa} = \frac{6328\times10^{-10}\text{ m}}{2\sin 5.53\text{ deg}} = 3.28\times10^{-6}\text{ m}$$

Thus the velocity perpendicular to the fringes is

$$U(\text{m/s}) = fd_f = f(3.28\times10^{-6})\quad f = \text{Doppler frequency (Hz)}$$

Because of the difference in refractive indices between air and the plexiglass (1.49), there existed the need to locate the crossing point of the two beams, or the measuring point. In the experiment, determination of the measuring position was carried out with a position finder, which is a semitransparent plate with marked coordinates, supported by a plexiglass holder. Before any point velocity was measured, the position finder was pushed into the combustion chamber model to obtain the exact coordinates of the beam crossing point.

Since a standard laser anemometer system has a 180-deg directional ambiguity, the frequency shifting was necessary to distinguish the flow direction. A TSI 982-2 acousto-optic (Bragg) cell was used to provide one beam with a frequency shift of 40 MHz, and the downmix circuit (TSI model 9186 frequency shifter) permitted a decrease of the effective frequency shift to a desirable level. In this experiment, 2 MHz (corresponding to 6.567 m/s velocity shifting) was selected for the axial velocity measurements. This selection of 2 MHz was based on the estimate that the reverse flow was much smaller than 6.567 m/s. As for the radial direction, the selection of frequency shift required more elaborate considerations. First we needed to compute the time for a particle to pass the center of the measuring volume (100 fringes) at 5 MHz, corresponding to 16.417 m/s, which approximated the maximum axial velocity. The output frequency was processed with a TSI 1980 counter that was set to allow eight cycles to validate a frequency reading. If the radial velocity were zero, the minimum frequency shifting required to obtain a valid reading would be

$$f_s = 8\text{ cycles}/20\,\mu\text{s} = 0.4\text{ MHz}$$

Therefore, in order to distinguish a 2-MHz equivalent reverse velocity ($\sim$6.57 m/s), the minimum required frequency shifting should be

$$f_s \simeq 0.4\text{ MHz} + 2\text{ MHz} = 2.4\text{ MHz}$$

To be consistent with the conservatism, a 5-MHz shifting was selected for the radial velocity measurements. The receiving optical package consisted of a 25-cm focal-length lens, a concave lens, and a 45-deg mirror to reflect the collected light into a photomultiplier in order to increase the signal-to-noise ratio by blocking the extraneous light. Then the counter converted the shifted Doppler signals into analog voltages. A digital readout device also gave a direct readout for velocity conversion and the data rate (data accepted by timer module logics per second). A TSI 1076 rms meter was used for measuring the rms value of the analog output from the counter.

A pressure transducer with a full range of 10 g/cm^2 (model PG-C, Kyowa) was used for static pressure measurements along the wall of the combustion chamber. The transducer is a strain-gage type with a pressure/strain ratio of 0.004198 g/cm^2/1.0$\times10^{-6}$. To measure pressure, the transducer was connected to each pressure tap on the model and the mean voltage was read. The output voltage was subsequently converted into the actual pressure.

Experimental Procedure

For axial velocity measurements, the plane of laser beam crossing was set to be horizontal by rotating the beamsplitter and the Bragg cell. After the mean and rms value at a measuring point were recorded, the combustion chamber model was then moved to a new position, for the next measuring point, by adjustment of the wooden model holder.

Velocity measurements were carried out at 2-cm intervals in the axial direction, beginning at $x = 3$ cm. For the radial cross section, data were taken at 0.5-cm intervals beginning at the centerline, $r = 0$.

After completion of the axial velocity measurements, the plane of the laser beams was rotated to be vertical. Then the radial velocity measurements proceeded as those for the axial direction. To obtain the Reynolds stresses, measurements of velocity fluctuations at ±45 deg were required. $\bar{e}^2_+$ and $\bar{e}^2_-$ are

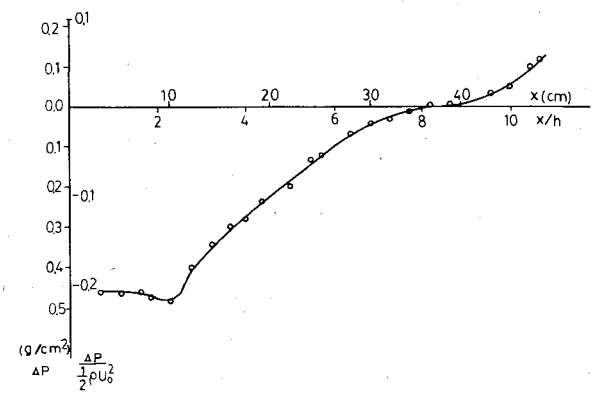

Fig. 4 Distribution of pressure along the wall.

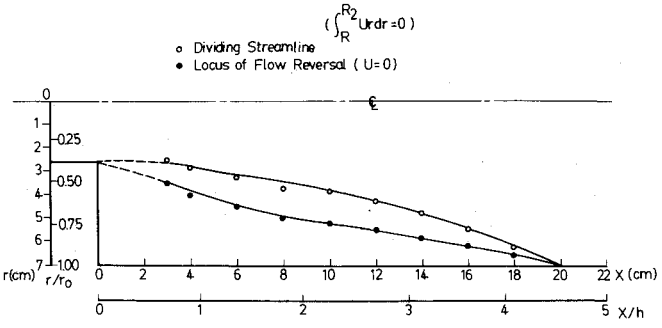

Fig. 5 Observed recirculation zone and dividing streamline.

the mean squares of the total velocity fluctuations in +45 deg and −45 deg, respectively. Then the Reynolds stresses can be obtained from the simple algebraic relation

$$\overline{uv} = \tfrac{1}{2}(\bar{e}_+^2 - \bar{e}_-^2)$$

III. Results and Discussion

Wall Pressure Distribution

The distribution of measured static pressures along the wall is plotted in Fig. 4. The axial distance has been normalized with the step height h. The pressure is normalized with the kinetic energy at the inlet, and the reference pressure is atmospheric pressure. There is a slight decline in pressure after the enlargement. The relative minimum is located near $x/h = 2.3$, then a rapid rise in pressure follows. The zero crossing occurs at about 8.5 step heights. This tendency is in agreement with the work of Teyssandier and Wilson,[6] who conducted measurements on various enlargement conditions in pipes.

Determination of Dividing Streamline and Flow Reattachment Point

The connecting points for the axial flow to reversal ($U=0$) are shown in Fig. 5. The same figure shows the dividing streamline, which is defined as the line at which there is zero net flow between it and the wall. A mathematical expression can be written

$$\int_R^{R_2} Ur\,dr = 0$$

where R is the point through which the dividing streamline passes and R_2 is the radius of the combustion chamber. This dividing streamline is usually considered to be the boundary that separates the recirculation zone from the main flow.

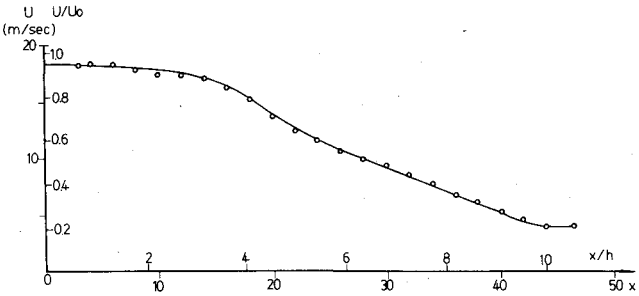

Fig. 6 Centerline profile of the mean axial velocity.

The reattachment point is estimated to be $x = 20$ cm from Fig. 5, and the reattachment length is about 4.5 step heights. This result is different from the 6-9 step heights suggested by Moon and Rudinger[7] in an abruptly expanding circular duct for Reynolds numbers ranging from 10^3 to 10^6. The reason for the shorter reattachment length in the present study is thought to be the fact that a short, rapidly contracted nozzle followed the sudden enlargement, whereas Moon and Rudinger's work was conducted in a long pipe after a sudden expansion. The higher back pressure in the present study definitely contributed to the shorter reattachment length.

Mean-Velocity Characteristics

Figure 6 presents the centerline values of the mean axial velocities. The potential core was estimated to be 2.3 D_1 (D_1 is the inlet pipe diameter) in length. Mean velocity decayed linearly until it reached about 20% of the initial value, at a distance of $x/h = 10$ or $x/D_1 = 8.5$. A similar measurement was made by Lu,[8] who indicated that the central velocity decreased to 25% of the inlet velocity at a downstream distance of $x/D_1 = 8$. The greater decay rate in the present study was due to the larger expansion ratio, $D_2/D_1 = 2.69$, in comparison with a ratio of 2 in Lu's investigation. Thus, the initial flow penetrated less into the downstream in the present work.

The measured axial velocity components are plotted in Fig. 7. The flow pattern showed a distinct recirculating flow after the enlargement. It should also be noted that the maximum reverse velocity was located at about 2.3 step heights. The magnitude of this maximum reverse velocity was about 10% of the inlet velocity and about 12% of the center velocity at the same location. Prior to the reattachment point the velocity field showed a slow reverse flow; after this point the velocity field became more uniform. No similarity among these velocity profiles could be determined since there was hardly any time for the flow to recover before reaching the con-

The radial velocities are presented in Fig. 8. These radial velocity profiles suggest that the radial flow spreads from the center part toward the wall. Because of the abrupt enlargement, the spread rate was high in the recirculation zone, especially near the reattachment region. The maximum radial velocity was found between $x = 4.1$ and $4.5h$, where the reattachment point was located. The radial velocity at these two points was about $0.31U_0$. Further downstream from the reattachment point, the radial velocity decreased gradually. It became negligible after two reattachment lengths.

Isopleths of turbulent kinetic energy, defined as $\frac{3}{4}(\bar{u}^2 + \bar{v}^2)$, and mean velocity $\sqrt{U^2 + V^2}$ are plotted in Fig. 9. It is noted that the maximum turbulent kinetic energy clearly followed the dividing streamline, where strong production of turbulence is expected. This will be pointed out again in the following subsection. The mean-velocity gradient was very high in the recirculation zone and around the inlet jet. These high gradients contributed to the rapid mixing in the thin shear layer.

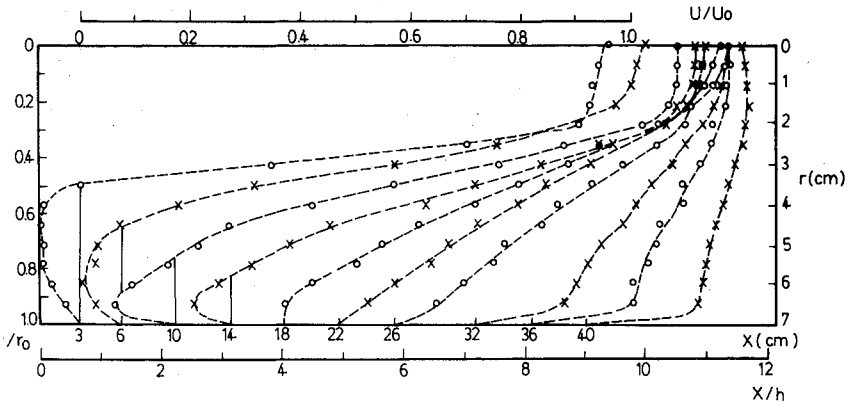

Fig. 7 Mean axial velocity profiles.

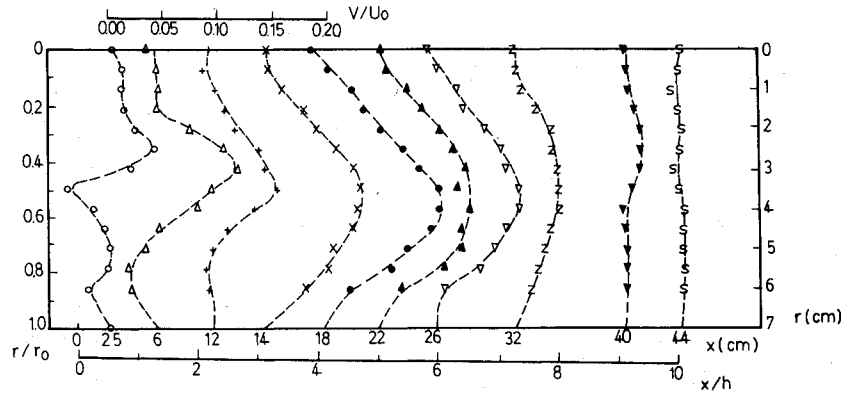

Fig. 8 Mean radial velocity profiles.

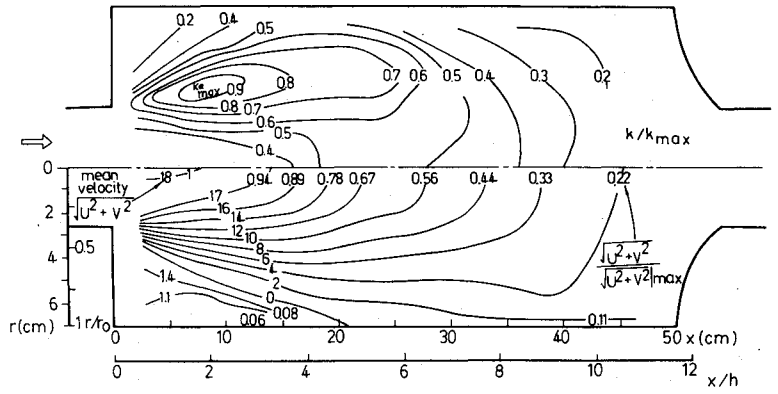

Fig. 9 Contours of mean velocity and turbulent kinetic energy.

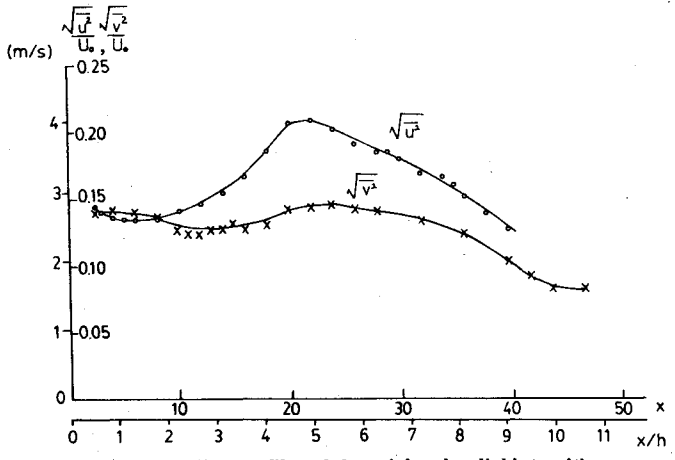

Fig. 10 Centerline profiles of the axial and radial intensities.

Turbulent Velocity Fluctuations

The measured axial and radial velocities, normalized with the inlet velocity U_0, are shown in Figs. 10-13. Naturally the turbulence was highly anisotropic near the reattachment region. Further downstream the two fluctuating components grow to similar magnitudes, with the axial fluctuation $\sqrt{\bar{u}^2}$ slightly greater than the radial function $\sqrt{\bar{v}^2}$. Sharp increases in $\sqrt{\bar{u}^2}$ and $\sqrt{\bar{v}^2}$ occurred in the abrupt-step dump. These fluctuations were greatly amplified in the shear layer region. This finding confirmed that considerable turbulent kinetic energy was being released.

The centerline axial and radial turbulence intensities are shown in Fig. 10. The maximum velocity fluctuations occurred immediately after the reattachment point. The maximum $\sqrt{\bar{u}^2}$ and $\sqrt{\bar{v}^2}$ values were 0.21 and $0.15U_0$, respectively. These values are, in general, in agreement with the data obtained by Chaturvedi,[9] who investigated the flow

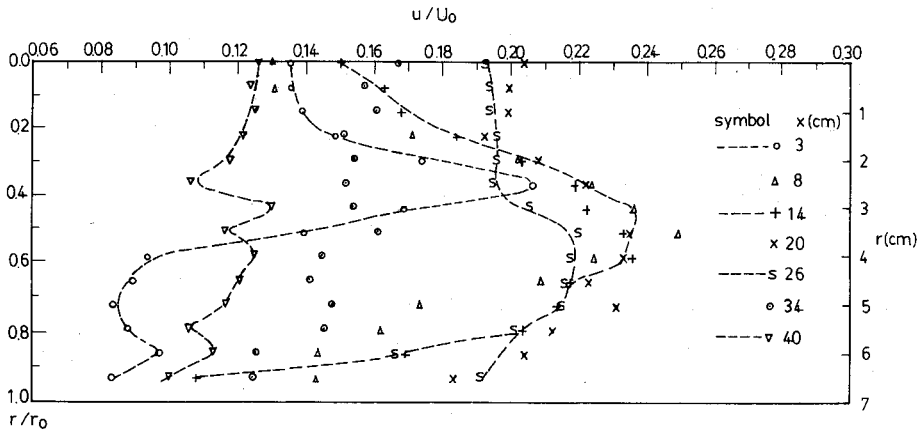

Fig. 11 Normalized turbulent intensities in the axial direction.

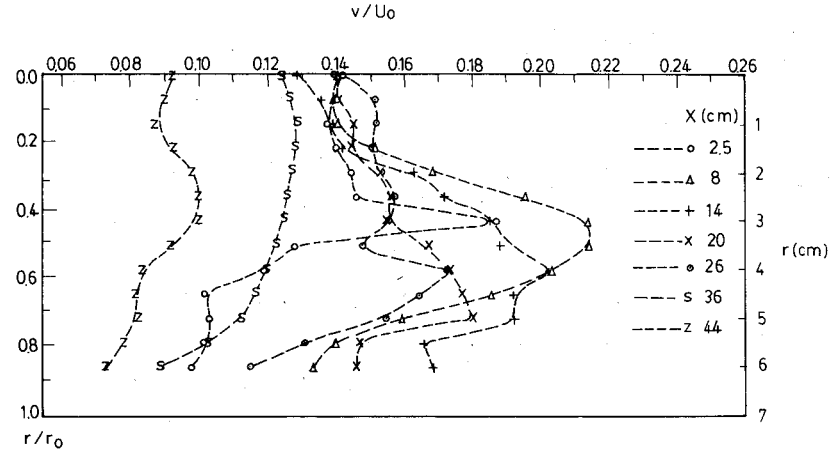

Fig. 12 Normalized turbulent intensities in the radial direction.

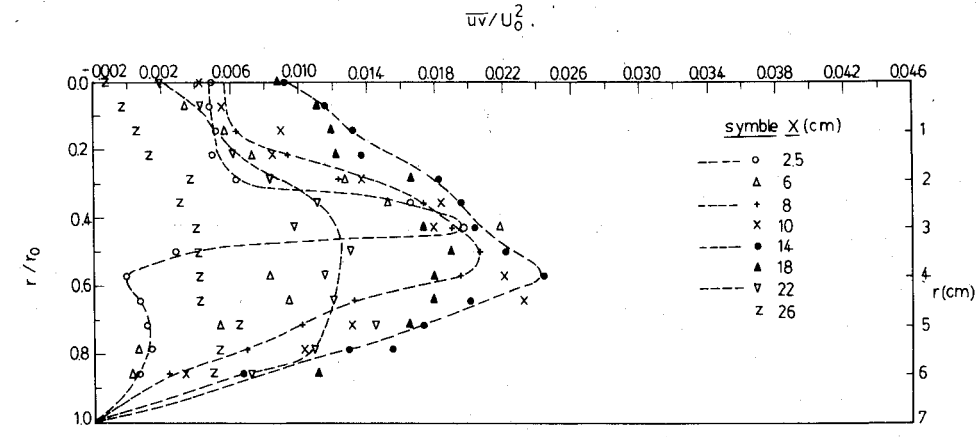

Fig. 13 Normalized Reynolds stress profiles.

characteristics of axisymmetric expansions with a hot-wire anemometer. The magnitude of fluctuation in the inlet and downstream regions is, however, higher than that found by Chaturvedi. The high relative turbulence intensity (0.13) in the inlet region was due to the lack of a screen in the inlet in this experiment. The turbulence intensities of the downstream region were about $0.08U_0$. In addition, with the aid of a Bragg cell, the LDA method is believed to generate a more desirable result, since a hot wire is essentially a "blind" instrument.

The turbulent energy contours shown in Fig. 9 are similar to those in Runchal's work,[10] in which a two-equation model (W model) was used for computing a pipe-expansion problem. The turbulent energy contours revealed that the shear layer, where high gradients of mean velocity occurred, was associated with high turbulent energy levels. The energy-containing eddies were highly diffusive in the recirculation zone. They were also convected by the slow mean motion and eventually dissipated into heat. Further downstream the turbulence intensity was smaller and generally showed a trend to isotropy.

The normalized Reynolds stresses of selected transverses are shown in Fig. 13. The high Reynolds stresses in the shear layer region are consistent with the proposal that Reynolds stress is proportional to the turbulent kinetic energy and velocity gradients. The general distribution of the Reynolds stresses is similar to Chaturvedi's findings.[9] The maximum value, occurring just after the abrupt step dump, was 0.0245. This value is of the same magnitude as that of a recirculation flow behind a disk, investigated by Durão and Whitelaw.[11] The nonzero values in the centerline (Fig. 13) may have been due to the combined system errors made during the separate measurement of $\bar{e}^2_+$ and $\bar{e}^2_-$.

Data Accuracy

Several aspects of the method of measurement could have affected data accuracy, although most of the induced errors were minimized when possible. First, the refractive index of plexiglass (1.49) is different from that of air. Refraction took place when the laser beams passed through the curved wall of the plexiglass model. The beam intersection angle (2κ) may change slightly if the two laser beams refract differently. This slight change of intersection angle was corrected using a simple computer program. Another effect of refraction was the limitation on measurements very close to the wall. In this study, the closest point measured was about 1.0 cm from the wall.

The second possible source of error was the inherent problem of seeding scatterers in the flow, since the LDA measures particle velocity, not fluid velocity. The scatterers chosen here were water droplets, because of health concerns. The particles were 3 μm or smaller in size. According to Chao,[12] these water droplets should be able to follow fluctuations in fluid velocity within 2% of its rms value at 1.5 kHz. Thus deviation of particle velocity from the true fluid velocity is not considered to be a matter of concern.

In order to increase the signal-to-noise level and reduce dropout time, the flow was continuously seeded and a closed loop was formed to conserve scatterers and to make sure a uniform distribution of scatterers was reached, to avoid the problem of velocity biasing. Although the flow was heavily seeded, the signal was still intermittent in some portions of the flowfield. The fact that the counter held the last reading when no acceptable signal was permitted helped considerably for mean-flow computations. As for rms measurements, the validity of assuming a continuous analog signal depended on the data rate. If the data rate was low, the analog output (in proportion to the instantaneous Doppler frequencies) appeared as a series of square waves of varying amplitudes and periods. The lower the data rate, the longer the periods of the analog output and the greater the error of the rms output. In the experiment, the data rates were about 10^2 readings/s near the wall and usually about 10^3 readings/s near the central part of the combustion chamber model. The combined errors from refraction and from the data rate favor measurement accuracy near the center of the chamber.

From the view of flow rate conservation, the integrations of the mean axial velocity

$$\int_0^{R_2} Ur\,dr$$

for each transverse section are constant. In this study, the integrated flow rates, calculated numerically using the experimental data, were within 6.5%.

IV. Conclusions

The following conclusions can be made in view of this experimental study:

1) The laser-Doppler anemometer with a frequency shifter is a useful instrumentation for measuring reverse flowfields. Especially for the highly turbulent flowfield encountered in this study, measurements from a conventional hot-wire anemometer may present considerable errors.

2) The flow characteristics of the combustion chamber model are quantitatively similar to pipe-expansion flow except in the downstream region. The reattachment length, $x/h = 4.5$, in this investigation is shorter than that of suddenly expanded pipe flow.

3) The potential core of the inlet jet is estimated to be $2.3D_1$ (12 cm) in length. The centerline velocity decays almost linearly until it reaches about 20% of the initial value at 10 step heights. The larger the expansion ratio, the faster the central velocity decreases.

4) Prior to the reattachment point, the flow profiles show a gradual return toward the upstream region in the recirculation zone. After this point, the velocity profile becomes more uniform. No similarity among these velocity profiles can be determined. The maximum velocity fluctuations along the centerline occur immediately after the reattachment point.

5) The turbulent energy contours reveal that the shear layer, where the high gradient of mean velocity occurs, is associated with high energy levels. Thus the maximum turbulent zone overlaps the dividing streamline.

6) The high turbulent kinetic energy, produced by large velocity gradients in the shear layer, is transported by both diffusion and convection in and out of the recirculation zone. The flowfield is anisotropic in the recirculation zone and gradually becomes more isotropic after the reattachment point.

7) Because of the necessary seeding in the experiment, the data rate favors measurement accuracy near the center of the chamber.

References

[1] Belding, J. A. and Coley, W. B., "Integral Rocket/Ramjets for Tactical Missiles," *Astronautics and Aeronautics,* Vol. 11, Dec. 1973.

[2] Drewry, J. E., "Fluid Dynamic Characterization of Sudden-Expansion Ramjet Combustor Flowfields," *AIAA Journal,* Vol. 16, April 1978, pp. 313-319.

[3] Bradshaw, P. and Wong, F. Y. F., "The Reattachment and Relaxation of a Turbulent Shear Layer," *Journal of Fluid Mechanics,* Vol. 52, Pt. 1, 1972, p. 116.

[4] Back, L. H. and Roschke, E. J., "Shear-Layer Flow Regimes and Wave Instabilities and Reattachment Lengths Downstream of an Abrupt Circular Channel Expansion;" *Journal of Applied Mechanics, Transactions of ASME,* Sept. 1972, pp. 677-681.

[5] Thomas, A. N., "New-Generation Ramjets—A Promising Future," *AIAA Journal,* Vol. 18, June 1980, p. 36.

[6] Teyssandier, R. C. and Wilson, M. F., "An Anaysis of Flow Through Sudden Enlargements in Pipes," *Journal of Fluid Mechanics,* Vol. 64, Pt. 1, 1974, pp. 85-95.

[7] Moon, L. F. and Rudinger, G., "Velocity Distribution in an Abruptly Expanding Circular Duct," *Journal of Fluids Engineering, Transactions of ASME,* March 1977, pp. 226-230.

[8] Lu, C. C., "Measurements of Turbulent Flow Velocity for Sudden Expansion Cylindrical Tube Using Laser Doppler Velocimeter (LDV)," *AIChE Journal,* Vol. 26, March 1980, pp. 303-305.

[9] Chaturvedi, M. C., "Flow Characteristics of Axisymmetric Expansions," *Journal of Hydraulics Division,* May 1963, pp. 61-92.

[10] Launder, B. E. and Spalding, D. B., *Lectures in Mathematical Models of Turbulence,* Academic Press, London and New York, 1972, p. 108.

[11] Durão, D. F. G. and Whitelaw, J. H., "Velocity Characteristics of the Flow in the Near Wake of a Disk," *Journal of Fluid Mechanics,* Vol. 85, 1978, pp. 369-385.

[12] Chao, B. T., "Turbulent Transport Behavior of Small Particles in Dilute Suspension," *Osterreichisches Ingenieur-Archiv,* Vol. 18, 1964.